Single-Component Donor–Acceptor Organic Semiconductors Derived from TCNQ

Paloma Bando, Nazario Martín,* José L. Segura, and Carlos Seoane*

Departamento de Química Orgánica, Facultad de Química, Universidad Complutense, E-28040 Madrid, Spain

Enrique Ortí, Pedro M. Viruela, and Rafael Viruela

Departamento de Química Física, Universidad de Valencia, E-46100-Burjassot (Valencia), Spain

Armando Albert and Félix H. Cano

U.E.I Cristalografía, Instituto "Rocasolano", CSIC, Serrano 116, E-28006-Madrid, Spain

Received April 27, 1994®

13,13,14,14-Tetracyanobenzo[*b*]naphtho[2,3-*e*][1,4]dithiin-6,11-quinodimethane (**9a**) and 13,13,14,14-tetracyanobenzo[*b*]naphtho[2,3-*e*][1,4]oxathiin-6,11-quinodimethane (**10a**) and their methyl-substituted derivatives (**9b** and **10b–d**, respectively) have been prepared as single-component donor-acceptor compounds from the corresponding quinones **7** and **8** by using the Lehnert's reagent. UV–vis spectra of the novel compounds reveal the presence of an intramolecular electronic transfer from the donor to the acceptor moiety. Cyclic voltammetry displays, in addition to the oxidation peak, a two-electron reduction wave to the dianion, as confirmed by controlled potential coulometry analysis. The crystallographical study carried out on single crystals of compound **10d** shows that molecules are not planar and stack with aromatic interactions between donor and acceptor moieties. In agreement with the crystallographical results, the electrical conductivity measured on a powder sample of **10c** exhibits semiconductive behavior. Molecular orbital calculations using the PM3 semiempirical method were performed on both neutral and oxidized/reduced compounds and predict that molecules are severely distorted from planarity. Distortions are compared with crystallographic data and are analyzed in terms of nonbonding interactions and crystal packing. Valence effective Hamiltonian (VEH) nonempirical calculations were used to study the electronic properties and support the intramolecular charge-transfer nature of the lowest-energy absorption band. The evolution of the geometric structure evidences a gain of aromaticity upon oxidation and reduction that justifies the obtention of stable cations and anions. The observation of a unique two-electron reduction wave to the dianion is rationalized by comparing the electronic and structural changes induced by reduction on compound **9a** and on the parent TCNQ molecule.

Introduction

In recent years considerable attention has been directed toward molecular structures exhibiting electrical properties in the solid state.[1] This effort has allowed the establishment of some of the electronic and structural requirements to form electrically conducting materials.[2] Planar molecules with delocalized π-electronic structures in the donor (D) and acceptor (A) moieties and a partial degree of electronic transfer between them are among the necessary conditions to form conducting segregated stacks.[2] Formation of charge-transfer complexes (CTC) is usually accompanied by a capricious donor (D)/acceptor (A) stoichiometric ratio. The synthesis of compounds of D-σ-A type, in which the donor and acceptor parts belong to the same organic molecule, overcomes these difficulties and allows to the the D/A stoichiometry to be fixed intramolecularly.[3]

Furthermore, D-σ-A structures are the base for the development of the "molecular electronics" to form metal–organic molecule–metal devices with an unidirectional electron flow,[4] for the design of artificial photosynthetic systems constituted by electron donor–spacer–electron acceptor compounds,[5] and for the obtention of molecular chromophores exhibiting large second-order nonlinear optical (NLO) response for which a strong intramolecular charge-transfer excitation is an indispensable prerequisite.[6]

On the other hand, organic compounds exhibiting semiconducting properties based on a single component have only recently been reported.[7] These compounds

® Abstract published in *Advance ACS Abstracts,* July 1, 1994.

(1) Cowan, D. O.; Wlygul, F. M. *Chem. Eng. News* **1986**, *64*, 28. Bryce, M. R. *Chem. Soc. Rev.* **1991**, *20*, 355. For an overview, see also the proceeding of the International Conference on Science and Technology of Synthetic Metals (ICSM): ICSM'90, *Synth. Met.* **1991**, *41-43*. ICSM92, *Synth. Met.* **1993**, *55–57*.

(2) Hünig, S; Erk, P. *Adv. Mater.* **1991**, *3*, 225. Becker, J. Y.; Bernstein, S; Bittner, S; Shaik, S. S. *Pure Appl. Chem.* **1990**,*62*, 467. Shaik, S. S. *J. Am. Chem. Soc.* **1982**, *104*, 5328.

(3) Becker, J. Y.; Bernstein, J.; Bittner, S.; Levi, N.; Shaik, S. S. *J. Am. Chem. Soc.* **1983**, *105*, 4468. Becker, J. Y.; Bernstein, J.; Bittner, S.; Levi, N.; Shaik, S. S. *J. Org. Chem.* **1988**, *53*, 1689.

(4) Metzger, R. M.; Panetta, Ch. *New J. Chem.* **1991**, *15*, 209 and references cited therein. See also: *Molecular Electronic-Science and Technology*; Aviram, A., Ed.; Engineering Foundation: New York, 1989.

(5) *Photoinduced Electron Transfer*; Fox, M. A., Chanon, M., Eds.; Elsevier: Amsterdam, 1988 and references cited therein. Danielson, E.; Elliot, C. M.; Merkert, J. N.; Meyer, T. J. *J. Am. Chem. Soc.* **1987**, *109*, 2519. Wasielewski, M. R.; Niemczyk, M. P; Svek, W. A.; Pewitt, E. B. *J. Am. Chem. Soc.* **1985**, *107*, 5562. Cowan, J. A.; Sanders, J.; Beddard, G. S.; Harrison, R. J. *J. Chem. Soc., Chem. Commun.* **1987**, 55. Gust, D.; Moore, T. A. *Science* **1989**, *244*, 35. Larson, S. L.; Cooley, L. F.; Elliot, C. M.; Kelley, D. F. *J. Am. Chem. Soc.* **1992**, *114*, 9504. Tamiaki, H.; Maruyama, K. *J. Chem. Soc., Perkin Trans. 1* **1992**, 2431.

0022-3263/94/1959-4618$04.50/0

Scheme 1

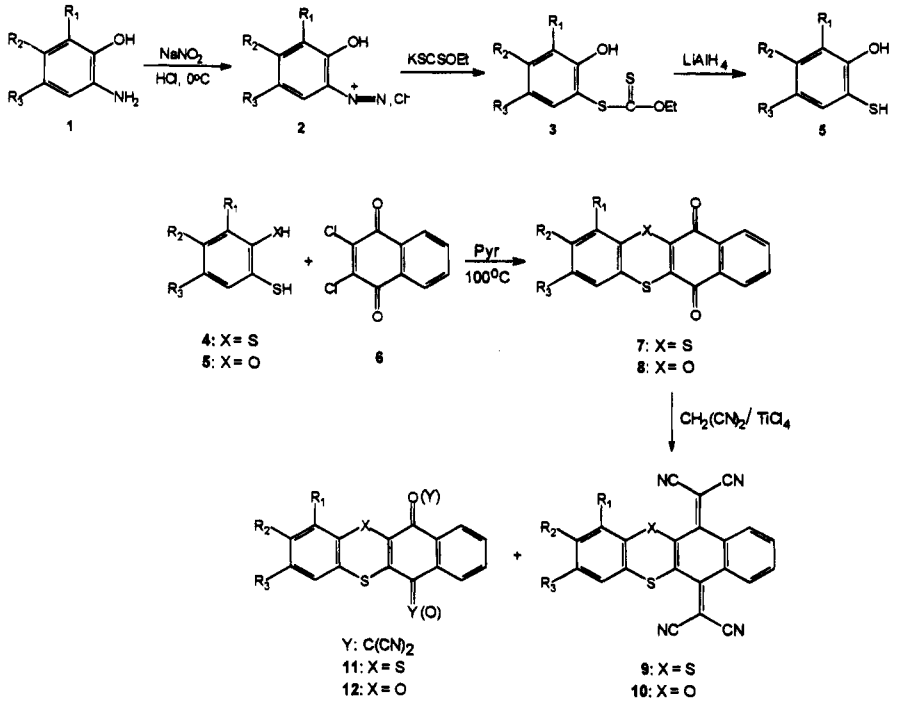

involve mainly tetrathiafulvalene (TTF) derivatives containing long alkyl chains or methyltelluro substituents in which strong intermolecular interactions take place.[8] Good conductivities have also been found in stable heterocyclic biradicals such as 1,4-phenylenebis(diselenadiazolyl)[9] and neutral radicals containing the pyrazino-TCNQ structure.[10]

In this paper, we describe a new type of single component donor–acceptor organic compounds in which the donor and acceptor moieties are linked by two sulfur (or sulfur/oxygen) atoms.[11] We combine the results of experimental UV–vis, cyclic voltammetry, and X-ray crystallographic measurements and the results of quantum-chemical calculations carried out within the MNDO-PM3 (modified neglect of diatomic overlap, parametric method number 3) and VEH (valence effective Hamiltonian) methodologies. The target molecules present the following advantages: (a) The molecule contains a prefixed D:A stoichiometric ratio, and consequently, it would be possible to tune the electron transfer degree using different substituents. (b) The presence of two heteroatom bridges overcomes the orthogonal relative geometry between donor and acceptor moieties found when only one bridge is present.[12] (c) The crystal packing in the solid state can be modified by changing the intramolecular connectivity. (d) The benzene ring fused to the tetracyano-*p*-quinodimethane (TCNQ) moiety is useful in decreasing on-site Coulombic repusions.[13] (e) Finally, the presence of one or two sulfur atoms in the molecule may reinforce the intermolecular interactions in the solid state.[14]

Results and Discussion

Synthesis. The preparation of the target molecules **9** and **10** was carried out by reaction of benzo[*b*]naphtho-[2,3-*e*][1,4]dithiin-6,11-quinones **7**[15] and benzo[*b*]naphtho-[2,3-*e*][1,4]oxathiin-6,11-quinones **8** with malononitrile by using the Lehnert reagent[16] to give the respective TCNQ derivatives **9** and **10**.

The synthesis of the starting quinones involves a multistep process. The preparation of quinones **7** was carried out by reaction of 2,3-dichloronaphthoquinone (**6**) with the corresponding substituted benzenedithiols (**4**), available from commercial sources, by following an improved procedure of the previously described method[15] (Scheme 1).

Benzo[*b*]naphtho[2,3-*e*][1,4]oxathiin-6,11-quinones **8** were obtained by reaction of 2,3-dichloronaphthoquinone

(6) Boyd, R. W. *Nonlinear Optics*; Academic Press: New York, 1992. Prasad, P. N.; Williams, D. J. *Introduction to Nonlinear Optical Effects in Molecules and Polymers*; Wiley: New York, 1991. Shen, Y. R. *The Principles of Nonlinear Optics*; Wiley: New York, 1984. See also: Di Bella, S.; Fragalá, I. L.; Rattner, M. A.; Marks, T. J. *J. Am. Chem. Soc.* **1993**, *115*, 682. Joshi, M. V.; Cava, M. P.; Lakshmikantham, M. V.; Metzger R. M.; Abdeldayem, H.; Henry, M.; Venkateswarly, P. *Synth. Met.* **1993**, *57*, 3974.

(7) Yamashita, Y.; Tanaka, S.; Imaeda, K.; Inokuchi, H.; Sano, M. *J. Org. Chem.* **1992**, *57*, 5517.

(8) Inokuchi, H.; Saito, G.; Wu, P.; Seki, K.; Tang, T. B.; Mori, T.; Imaeda, K.; Enoki, T; Higuchi, Y.; Inaka, K.; Yasuoka, N. *Chem. Lett.* **1986**, 1263. Inokuchi, H.; Imaeda, K.; Enoki, T.; Mori, T.; Maruyama, Y.; Saito, G.; Okada, N.; Yamochi, Y.; Seki, K.; Higuchi, Y.; Yasuoka, N. *Nature* **1987**, *329*, 6134.

(9) Cordes, A. W.; Haddon, R. C.; Oakley, R. T.; Schneemeyer, L. F.; Waszczak, J. V.; Young, K. M.; Zimmerman, N. M. *J. Am. Chem. Soc.* **1991**, *113*, 582.

(10) Tsubata, Y.; Suzuki, T.; Miyashi, T.; Yamashita, Y. *J. Org. Chem.* **1992**, *57*, 6749.

(11) A part of this work was presented as a preliminary communication in the ICSM92, Göteborg, Sweden, 1992: *Synth. Met.* **1993**, *56*, 1721.

(12) Martín, N.; Segura, J. L.; Seoane, C.; Albert, A.; Cano, F. H. *J. Chem. Soc., Perkin Trans. 1* **1993**, 2363. See also ref 3.

(13) (a) Martín, N.; Hanack, M. *J. Chem. Soc., Chem. Commun.* **1988**, 1522. (b) Martín, N.; Behnisch, R.; Hanack, M. *J. Org. Chem.* **1989**, *54*, 2563. (c) Martín, N.; Navarro, J. A.; Seoane, C.; Albert, A.; Cano, F. H.; Becker, J. Y.; Khodorkovsky, V.; Harlev, E.; Hanack, M. *J. Org. Chem.* **1992**, *57*, 5726. (d) Cruz, P.; Martín, N.; Miguel, F.; Seoane, C.; Albert, A.; Cano, F. H.; González, A.; Pingarrón, J. M. *J. Org. Chem* **1992**, *57*, 6192.

(14) Kobayashi, K. *Phosphorus, Sulphur, Silicon* **1989**, *43*, 1987. Ogura, F.; Otsubo, T.; Aso, Y. *Pure Appl. Chem.* **1993**, *65*, 683.

(15) The synthesis of quinones **7** was carried out by a modification of the procedure described by: Gotarelli, G.; Lucarini, M.; Pedulli, G. F.; Spada, G. P.; Roffia, S. *J. Chem. Soc., Perkin Trans. 2* **1990**, 1519.

(16) Lehnert,W. *Tetrahedron Lett* **1970**, 4723. Lehnert, W. *Synthesis* **1974**, 667.

Table 1. Novel Compounds Prepared

compd	R_1	R_2	R_3	yield (%)	mp (°C)	λ_{max} (log ϵ)[a]	ν_{CN}[b]
7a[c]	H	H	H	73	288–290	542 (2.92)	
7b	H	Me	H	78	268–270	558 (2.93)	
8a	H	H	H	82	256–258	548 (2.94)	
8b	H	Me	H	91	244–246	560 (2.95)	
8c	H	H	Me	87	230–232	558 (2.97)	
8d	Me	H	Me	73	260–262	565 (2.98)	
9a	H	H	H	40	>300	515 (3.35)	2220
9b	H	Me	H	47	>300	528 (3.52)	2220
10a	H	H	H	37	>300	594 (3.42)	2222
10b	H	Me	H	41	>300	606 (3.45)	2215
10c	H	H	Me	46	>300	603 (3.43)	2220
10d	Me	H	Me	52	>300	621 (3.29)	2220

[a] In nm. Solvent: $CHCl_3$. [b] In KBr pellets (cm^{-1}). [c] Reference 15.

Chart 1

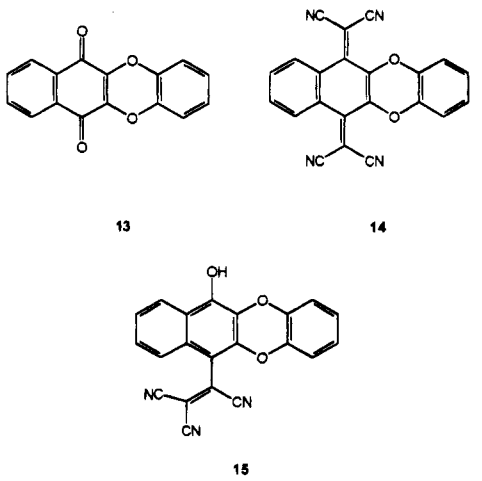

13 14 15

(**6**) with the substituted *o*-thiophenols (**5**) which were previously prepared from the corresponding *o*-aminophenols (**1**) by diazotization reaction, followed by formation of the xanthate (**3**) from the diazonium salt (**2**) by reaction with potassium ethyl xanthate. Further reduction of **3** with lithium aluminum hydride leads to the respective *o*-thiophenols (**5**)[17] (Scheme 1). The novel quinones **8** were thus obtained in high yields from **5** and **6**, using dry pyridine as solvent at 100 °C under argon atmosphere.

The reaction of quinones **7** and **8** with malononitrile in methylene dichloride and $TiCl_4$ in the presence of pyridine (Lehnert reagent)[16] yielded the novel heteroatom-substituted TCNQ derivatives **9** and **10** as dark blue, high melting point solids in moderate yields. The novel compounds thus prepared are listed in Table 1.

The dicyano derivatives **11** and **12** resulting from the monocondensation reaction could be isolated in some cases by fractional crystallization from the mother liquors, as a mixture of two constitutional isomers in lower yields. Formation of both isomers was ascertained by high-resolution ^{1}H-NMR spectra of the isomeric mixture. Attempts to separate them by flash chromatography were unsuccessful due to their instability on silica gel.

Additionally, depending on the reaction conditions (1:1.5 stoichiometric ratio for quinone:malononitrile and shorter reaction times) it is also possible to form the monocondensated compound as the major reaction product but in low to moderate yield.

(17) Djerassi, C.; Gorman, M.; Markley, F. X.; Oldenburg, E. B. *J. Am. Chem. Soc.* **1955**, *77*, 568.

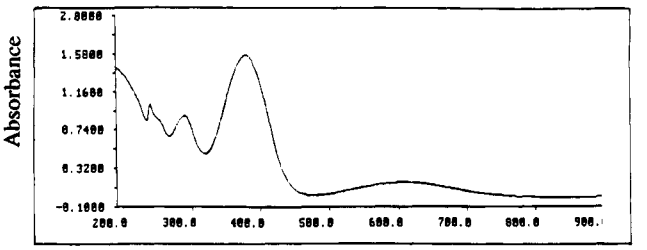

Figure 1. UV–vis spectrum of compound **10b** in $CHCl_3$.

Table 2. Cyclic Voltammetry Data of Novel D–A compounds (V vs SCE)[a]

compd	$E_{1/2}^{ox}$	$E_{1/2}^{1,red}$	$E_{1/2}^{2,red}$	ΔE	log K
7a	+1.41	−0.53	−1.09	0.56	9.49
7b	+1.35	−0.54	−1.09	0.55	9.32
8a	+1.52	−0.59	−1.09	0.50	8.47
8b	+1.44	−0.60	−1.13	0.53	8.98
8c	+1.47	−0.60	−1.11	0.51	8.64
8d	+1.42	−0.62	−1.11	0.49	8.30
9a	+1.39	−0.04			
9b	+1.61	−0.04			
10a	+1.57	0.00			
10b	+1.53	−0.01			
10c	+1.70	−0.01			
10d	+1.54	−0.01			
TCNQ[b]		+0.22	−0.35	0.57	9.66

[a] Electrolyte $Bu_4N^+ClO_4^-$; solvent CH_2Cl_2; scan rate 50 mV s^{-1}. [b] Measured in the same experimental conditions.

It is worth mentioning that previous attempts[18] to prepare the TCNQ derivatives **14** from benzo[*b*]naphtho-[2,3-*e*][1,4]dioxin-6,11-quinones (**13**) were unsuccessful, leading to the tricyano derivative **15** instead of the expected TCNQ derivative **14** (Chart 1). Substitution of one or both oxygen atoms by sulfur atoms in the dioxin-6,11-quinone (**13**) results in a favored 1,2-addition of malononitrile to both carbonyl groups in compounds **7** and **8**. The reaction of quinones with nucleophilic agents is not very well documented in the literature, and it has recently been reviewed from the standpoint of modern mechanistic ideas.[19]

The electronic spectra of quinones **7** and **8** and TCNQ derivatives **9** and **10** show, in addition to the expected bands in the UV region, the presence of a charge-transfer band as a low-energy absorption in the visible region which is shifted bathochromically when the donor fragment bears electron-releasing methyl groups (see Figure 1, Table 1). This feature suggests an intramolecular electron transfer from the donor to the acceptor part of the molecule. The intramolecular character of this electronic transition was confirmed by dilution experiments in the UV–vis spectra.

Electrochemistry. Cyclic voltammetry (CV) measurements on the novel compounds were carried out in methylene dichloride at room temperature with tetrabutylammonium perchlorate as the supporting electrolyte. The half-wave redox potentials measured are listed in Table 2. All compounds show the presence of an oxidation potential at positive values due to the oxidation of the oxathiin and dithiin groups which give rise to stable cation radicals. Interestingly, compounds **9** and **10**

(18) Czekanski, T.; Hanack, M.; Becker, J. Y.; Bernstein, J.; Bittner, S.; Kaufman-Orenstein, L.; Peleg, D. *J. Org. Chem.* **1991**, *56*, 1569.
(19) Kutyrev, A. A. *Tetrahedron* **1991**, *47*, 8043. See also: The Chemistry of the Quinoid Compound; Patai, S., Rappoport, Z., Eds.; Wiley: New York, 1988.

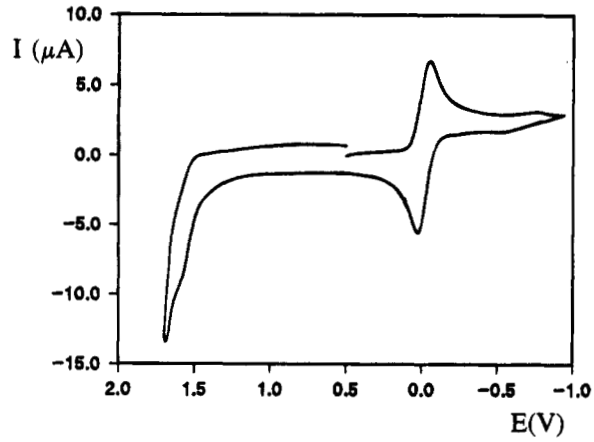

Figure 2. Cyclic voltammogram of compound **10b.**

exhibit only one electron reduction wave with a value intermediate between those of the parent TCNQ molecule (+0.22 and −0.35 V). The separation between the anodic and cathodic peaks, less than 60 mV, suggests a two-electron transfer to form the dianion (Figure 2). This finding was confirmed by controlled potential coulometric analysis for compound **10d** using a platinum sheet macroelectrode. Thus, the reduction wave of these compounds is indicative of an overall process leading to the dianion ($A + 2e^- \rightleftarrows A^{2-}$). This result is in good agreement with those reported for other π-extended TCNQ derivatives which exhibit a two-electron reduction single wave to the dianion.[20] ESR studies carried out on these TCNQ derivatives suggest that a coproportionation reaction ($A + A^{2-} \rightleftarrows 2A^{-}$) could also take place to some extent.[20c]

Compounds **9** show a slightly poorer electron-acceptor ability than compounds **10**, and the presence of methyl groups as substituents in **9** and **10** does not seem to alter significantly the reduction potential values (see Table 2).

The presence of heteroatoms (O, S) linked to the TCNQ ring has a remarkable effect on the electrochemical behavior of the tetracyclic molecules **9** and **10** which exhibit a two-electron single wave reduction. This finding contrasts with that observed for the tetracarbocyclic 13,13,14,14-tetracyano-5,12-naphthacenequinodimethane which shows two quasireversible reduction waves to the radical anion and dianion.[13b]

The cyclic voltammograms of starting quinones **7** and **8** exhibit, in addition to the oxidation peak at positive values, two single one-electron reduction waves to the corresponding radical anion and dianion. As expected, the values of the first reduction potential show the poorer acceptor ability of these compounds compared to their respective TCNQ derivatives **9** and **10**. (see Table 2).

The thermodynamic stability of the anion-radical in a two-step reduction process can be determined from log K, K being the disproportionation constant for the equilibrium $2A^- \rightleftarrows A + A^{2-}$. The values of log K (Table 2) are calculated from the difference between the two first reduction potentials ($\Delta E = E_{1/2}^{1,red} - E_{1/2}^{2,red}$).[21] Following this procedure, the stability of the anion-radical of quinones **7** is estimated to be similar to that of $TCNQ^{-}$

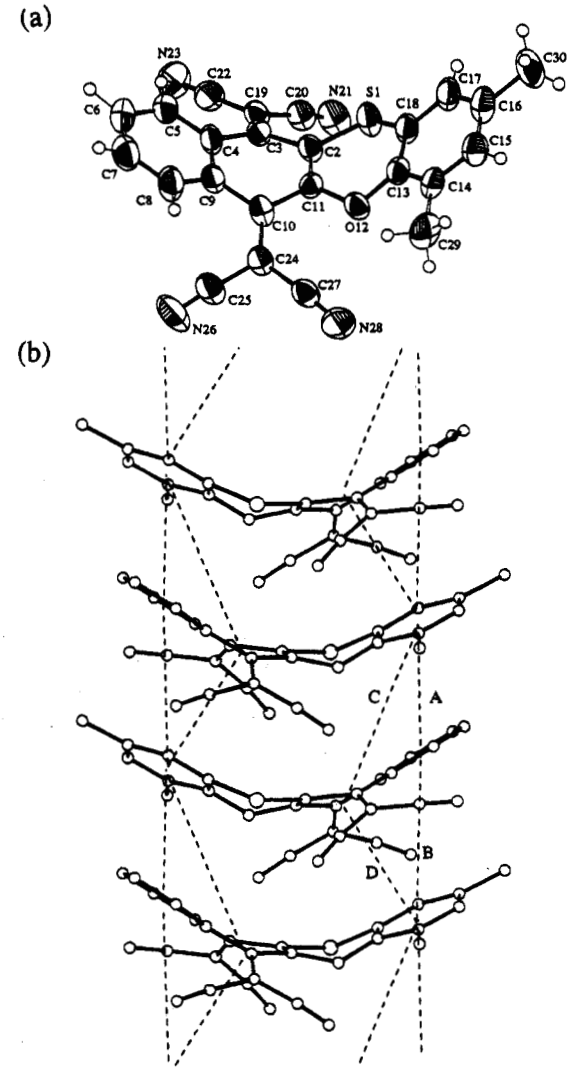

Figure 3. (a) Molecular structure of the compound, showing the atomic numbering. (b) The stacking along the b axis: ANG(A) = 4.01°, DZ(A) = 3.12 Å, DXY(A) = 2.52 Å; ANG(B) = 4.85°, DZ(B) = 3.67 Å , DXY(B) = 3.17 Å; ANG(C) = 5.26°, DZ(C) = 3.61 Å, DXY(C) = 3.83 Å; ANG(D) = 4.12°, DZ(D) = 3.91 Å, DXY(D) = 1.30 Å. ANG is the angle between aromatic rings, DZ is the distance from one centroid to the LS plane of the other ring, and DXY is the distance between one centroid and the projection of the other onto the first LS plane. These stacked chains form a two-dimensional close-packed pattern in the a–c projection.

and slightly higher than that of quinones **8**. The lower stability of the anion-radical for compounds **9** and **10** results from the observation that the first and second reduction waves coalesce into a single two-electron reduction wave.

Structural Study. The molecular structure of compound **10d** is shown in Figure 3, together with the atomic numbering scheme. The X-ray structural analysis performed on a single crystal shows that the molecule is not planar, with the TCNQ (C3, C10) and [1,4]oxathiin rings (S1, O12) displaying boat conformations. It is possible to set three planes along the molecule and to define the planarity in terms of the angles between these planes, i.e., the angles formed by the central plane (defined in average by atoms S1, C2, C3, C10, C11, O12) and the two external planes (from C3 to C10 and from O12 to S1) (see Figure 3). These angles have values of 152.8 (1) and 147.3 (1)°, respectively. The disposition of the

(20) (a) Aumüller, A.; Hünig, S. *Liebigs Ann. Chem.* **1984**, 618. (b) Ong, B. S.; Keoshkerian, B. *J. Org. Chem.* **1984**, *49*, 5002. (c) Kini, A. M.; Cowan, D. O.; Gerson, F.; Möckel, R. *J. Am. Chem. Soc.* **1985**, *107*, 556. (d) Martín, N.; Seoane, C.; Segura, J. L.; Marco, J. L.; Hanack, M. *Synth. Met.* **1991**, *42*, 1873.

(21) Jensen, B. S.; Parker, V. D. *J. Am. Chem. Soc.* **1975**, *97*, 5211.

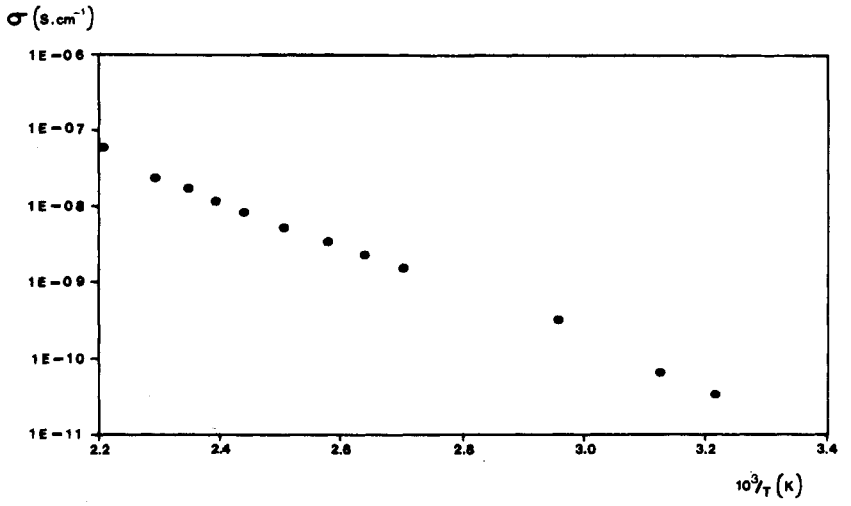

Figure 4. Temperature dependence of the electrical conductivity of compound **9b**.

dicyanomethylene groups is quite similar to that found in analogous acceptor molecules previously reported.[22]

As depicted in Figure 3, the crystal packing presents a stacking pattern of aromatic interactions along the *b* axis between donor and acceptor moieties.[23,24] The low overlapping of the rings involved in these interactions could be due to the steric hindrance between the cyano and methyl groups in **10d**. Interestingly, no S–S intermolecular interactions were observed due, probably, to the nonplanar geometry of the molecule.

The electrical conductivity measured for compressed powder pellets of compound **9b** by a two-probe technique was 10^{-11} S cm^{-1} at room temperature. The temperature dependence of conductivity is presented in Figure 4 and shows a semiconductive behavior with an activation energy (E_a) of 0.55 eV. The conductivity increases linearly up to $\sigma = 10^{-7}$ S cm^{-1} at 180 °C, which is still high for a single component organic compound.

Theoretical Calculations. In order to rationalize the experimental results presented above, we have calculated the geometric structure and the electronic properties of quinones **7** and **8** and TCNQ derivatives **9** and **10** by using molecular-orbital quantum-chemical methods. In the following discussion we mainly focus on the results obtained for the donor–acceptor TCNQ derivatives **9** and **10**, the properties calculated for quinones **7** and **8** being mentioned only for the sake of comparison. The atomic numbering used in this section corresponds to that depicted in Figure 3.

Molecular Structure. The molecular geometries of compounds **7** to **10** were fully optimized using the PM3 semiempirical method. No symmetry restriction was assumed during optimization except for molecules **7a** and **9a** for which a C_s symmetry was imposed. Figure 5 displays the most significant bond lengths and bond angles computed for compound **10d**. This molecule is a good example to summarize the main theoretical trends calculated for the geometric structures of compounds **7**–**10** since it presents the most complex molecular

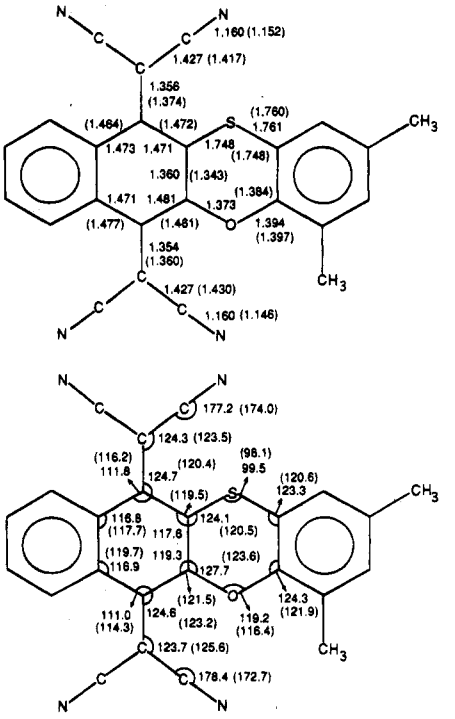

Figure 5. PM3-optimized bond lengths (top) and bond angles (bottom) calculated for **10d** (X-ray solid-state data are included in parentheses). Only the most relevant parameters are explicitly quoted. Bonds are in Å and angles in degrees.

structure (sterically hindered dicyano groups, two different heteroatom bridges, and two methyl groups). The X-ray geometric parameters obtained for **10d** are also included in Figure 5 to facilitate the comparison with experimental results.

As indicated in Figure 5, the two external benzene rings of **10d** preserve their aromaticity, all the carbon–carbon bonds having a length of 1.40 ± 0.10 Å and the internal bond angles being of 120 ± 1.0°. The central TCNQ ring also retains its quinoid character showing a high carbon–carbon bond-length alternation. The lengths obtained for bonds C2–C11 (1.360 Å), C2–C3 (1.471 Å), and C3–C19 (1.356 Å) are very similar to those calculated for the parent TCNQ molecule using the same methodology (1.345, 1.456, and 1.362 Å, respectively). The two heteroatom bridges defining the fourth ring of the molecule are significantly different from the structural

(22) Cruz, P.; Martín, N.; Miguel, F.; Seoane, C.; Albert, A.; Cano, F. H.; Leverenz, A.; Hanack, M. *Synth. Met.* **1992**, *48*, 59. Schubert, U.; Hünig, S.; Aumüller, A. *Liebigs Ann. Chem.* **1985**, 1216.

(23) Desiraju, G. R. *Crystal Engineering*; Elsevier: Amsterdam, 1989.

(24) Albert. A.; Cano, F. H. CONTACTOS, a Program for Systematical Study of Aromatic Ring Interactions, Instituto Rocasolano, C.S.I.C. Madrid, Spain, 1991. To be published.

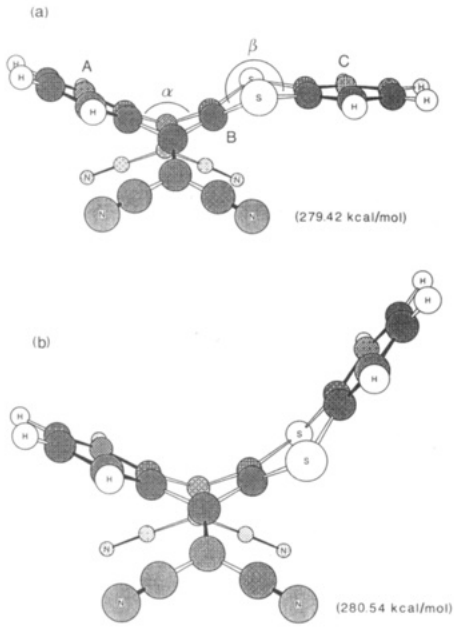

Figure 6. PM3-optimized minima calculated for **9a**. The respective heats of formation are indicated in parentheses. The most relevant molecular planes are labeled from A to C and the angles between them noted as α and β (see text for a complete definition).

standpoint. While the O12—C11, C13 bond distances (1.373, 1.394 Å) are considerably shorter than the S1—C2, C18 distances (1.748, 1.761 Å), the C11—O12—C13 bond angle (119.2°) is remarkably larger than the C2—S1—C18 angle (99.5°). These features determine important differences for the distances between the nonbonded atoms C2—C18 (2.891 Å) and C11—C13 (2.387 Å). All these trends stand for the whole set of molecules studied in this work and are supported by the crystallographic data measured for compound **10d** (see Figure 5). The average difference in absolute value between experimental and calculated geometric parameters is indeed only 0.01 Å for the bond lengths and of 2.7° for the bond angles. The difference is comparatively larger for the bond angles because theoretical calculations and X-ray analysis lead to different distortions from planarity as discussed below.

Theoretical calculations predict that the TCNQ derivatives **9** and **10** are severely distorted from planarity and that three different molecular planes could be defined for these compounds. These results are illustrated in Figure 6 for compound **9a** and agree with the X-ray structural analysis performed for **10d** (see Figure 3). The nonplanarity of TCNQ derivatives is mainly due to the strong steric interactions that take place between the cyano groups and the atoms in *peri* positions, i.e., the CH groups on the one side and the heteroatom bridges on the other side. To avoid these interactions both the TCNQ and the dithiin (**9**) or the oxathiin (**10**) rings are bent into a boat conformation, and the dicyanomethylene units are folded in the direction opposite to the bending of the TCNQ ring (see Figure 6). These distortions are identical to those reported for 11,11,12,12-tetracyano-9,10-anthraquinodimethane (TCAQ) for which the X-ray crystallographic analysis predicts a butterfly-type structure similar to those displayed in Figure 6 for compound **9a**.[25]

(25) Schubert, U.; Hünig, S.; Aumüller, A. *Liebigs Ann. Chem.* **1985**, 1216.

Table 3. PM3-Optimized angles (deg) formed by the principal molecular planes.[a] Experimental X-ray data are included in parenthese

molecule	α	β	γ
9a	134.6	202.8	43.9
9b	134.6	203.0	43.9
10a	136.7	191.4	42.9
10b	136.7	191.4	42.9
10c	136.7	191.4	42.8
10d	136.2 (152.8)[c]	182.0 (147.3)	42.9 (29.7)
TCAQ	138.3 (144.6)[b]		39.9 (30.4)
7a	142.9	202.3	32.2
8a	149.3	180.8	27.1
9,10-anthraquinone	156.1		19.6

[a] Angles α and β are defined in Figure 6 and correspond to those formed by molecular planes A and B and B and C, respectively. Angle γ is that formed by $C(CN)_2$ groups and the C2—C4—C9—C11 plane (see Figure 3 for numbering). [b] Reference 25. [c] This work.

Table 3 collects the theoretical values calculated for the angles describing the molecular distortion from planarity, i.e., the angles formed by the principal molecular planes. These planes correspond to those defined in the X-ray structural data section and are labeled in Figure 6a as follows: plane A fits that formed by atoms C3 to C10, plane B is the central plane constituted by atoms S1, C2, C3, C10, C11, and O12, and plane C comprises atoms O12 to C18 and S1. The angle formed by planes A and B is denoted α and that between planes B and C is called β. In addition, angle γ corresponds to that formed by the dicyanomethylene units and the C2—C4—C9—C11 plane and defines the bending of $C(CN)_2$ groups. The results obtained for TCAQ using the same methodology are included for the sake of comparison.

Angle α is calculated to have almost the same value for all the TCNQ derivatives listed in Table 3; i.e., it appears to be nearly independent of the presence and structure of the heteroatom bridges and of methyl substitution. The slight enlargement of angle α in going from **9a** (134.6°) to **10a** (136.7°) and from **10a** to TCAQ (138.3°) can be understood as a consequence of the size of the atom groups (S > O > CH) in the *peri* positions. The presence of two large sulfur atoms in **9a** determines the strongest steric interactions and therefore induces the highest folding. An equivalent trend is observed for angle γ, for which the maximum bending of the dicyanomethylene groups corresponds to compounds **9** (≈44°) with two sulfur atoms in *peri* positions, and the smallest value is found for TCAQ (≈40°). After these distortions, the distances between the cyano carbons and C5, C8 on one side and S1, S12 on the other side are 3.06 and 3.23 Å, respectively. In contrast with angle α, the values obtained for angle β depend on both the heteroatom bridges and the methyl substitution, and values of about 203 and 191° are, respectively, calculated for compounds **9** and **10**. Compound **10d** is an exception because the presence of the second methyl substituent in position R_1 determines an extra steric interaction with the neighboring cyano group which planarizes the dithiin ring (β = 182°).

When theoretically calculated molecular structures are compared with those obtained from X-ray solid-state data it should be borne in mind that theoretical calculations are performed on isolated systems without taking into account the forces involved in the crystal packing. In this way, the theoretical values calculated for angles α (136.2°) and γ (42.9°) of **10d** are in perfect agreement with those from X-ray data (152.8 and 29.7°, respectively)

since the packing forces tend to planarize the molecules in order to achieve the most compact crystal packing along the molecular stacks. This is also the case for TCAQ, for which the theoretical values ($\alpha = 138.3°$ and $\gamma = 39.9°$) are more distorted from planarity than the experimental ones ($\alpha = 144.6°$ and $\gamma = 30.4°$).[25] The molecular packing should be also invoked to explain the different orientation theoretically calculated and experimentally observed for plane C. Theoretically, it always points down ($\beta > 180°$) to the cyano groups (see Figure 6a and Table 3). Experimentally, it is found that plane C points up ($\beta < 180°$) in order to lie parallel to the acceptor moieties of the adjacent molecules along the stack (see Figure 3). Indeed, we have calculated for **9a** that the orientation with plane C pointing up ($\beta < 180°$) is also a minimum in the molecular potential energy surface and is only 1.12 kcal/mol higher in energy than the orientation with $\beta > 180°$ (see Figure 6). At the PM3 level, the barrier between these two minima is found to be almost nonexistent, the interconversion between them being therefore very easy since it implies an extra energy of only about 1 kcal/mol.

Table 3 also summarizes the distortions from planarity calculated for quinones **7** and **8** together with those obtained for the parent 9,10-anthraquinone. The PM3 results predict that the quinoid ring in **7** and **8** is less distorted than the TCNQ ring in **9** and **10**. This effect is clearly due to the weaker interactions that take place in quinones between the carbonyl groups and the groups in *peri* positions. The theoretical values obtained for angles α (**7a** < **8a** < 9,10-anthraquinone) and γ (**7a** > **8a** > 9,10-anthraquinone) follow the same trends discussed above for TCNQ derivatives and indicate that those interactions decrease in going from **7a** (S, S) to **8a** (S, O) and from **8a** to 9,10-anthraquinone (CH, CH). Angle β presents the same value for compounds **7a** and **9a** suggesting that the bending of the dithiin ring is an intrinsic feature and is not determined by the interaction with the cyano groups in compounds **9**. This is not the case for the oxathiin ring which is almost planar in **8a** ($\beta = 180.8°$) and presents some folding in **10a** ($\beta = 191.4°$) due to the interaction with cyano groups.

Electronic Structure. Molecular orbital calculations were performed on compounds **7**, **8** and **9**, **10** using the nonempirical quantum-chemical VEH technique and the PM3-optimized geometries. Compared to standard *ab initio* Hartree–Fock calculations, the VEH method yields molecular orbital energies of double-ζ quality and has the advantage of providing good estimates for the lowest energy optical transitions.[26,27]

Figure 7 displays the VEH atomic composition of the highest occupied molecular orbital (HOMO) and the lowest unoccupied molecular orbital (LUMO) calculated for compound **9a**. The HOMO is mainly localized on the donor benzodithiin environment, and the LUMO is spread over the acceptor TCNQ moiety. These topologies are found for all compounds listed in Table 1 and suggest that the HOMO → LUMO electronic transition implies an electron transfer from the donor part to the acceptor part of the molecule. For **9a**, this electronic transition is calculated to appear at an energy of 2.43 eV (510 nm) in perfect agreement with the lowest energy optical

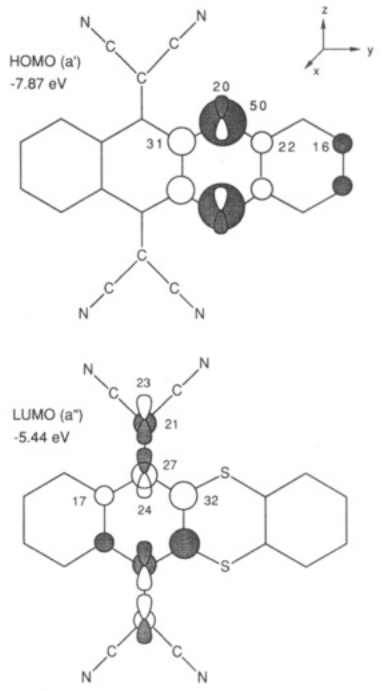

Figure 7. Energies, symmetries (C_s point group), and atomic orbital composition of the HOMO and LUMO of **9a**. The atomic orbital (AO) coefficients are given in units of 10^{-2}. Coefficients smaller than 0.15 are not indicated. Contributions from AOs other than p_x π-type orbitals are due to the nonplanarity of the molecule.

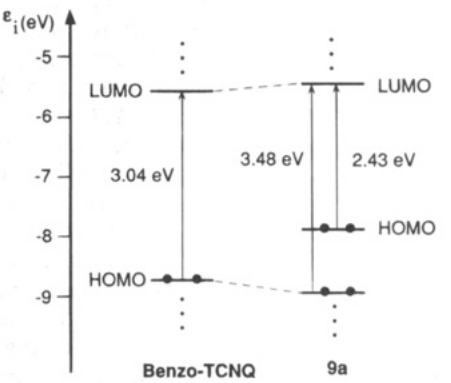

Figure 8. Calculated VEH one-electron energies (e_i) diagram showing the correlation between the highest occupied and lowest unoccupied molecular orbitals of benzo-TCNQ and **9a**.

absorption band observed experimentally (2.41 eV). Theoretical results therefore support the intramolecular charge-transfer nature of this absorption band. The symmetries of the HOMO (a′) and the LUMO (a″) predict that the charge-transfer band is polarized along the short molecular axis (z) in accord with that reported for similar naphthoquinone derivatives.[15] Dyes with short-axis polarized transitions are uncommon and could be used in liquid–crystal display technology as they produce two different colors depending on their alignment in liquid–crystalline matrices.[28]

The correlation diagram sketched in Figure 8 summarizes the effects of joining the donor benzodithiin moiety to the acceptor 9,9,10,10-tetracyano-1,4-naphthoquinodimethane (benzo-TCNQ) unit to obtain **9a**. The LUMO of benzo-TCNQ shows an atomic orbital composition similar to that of the LUMO of **9a** and is destabilized

(26) Brédas, J. L.; Thémans, B.; André, J. M. *J. Chem. Phys.* **1983**, *70*, 6137.
(27) Viruela-Martín, R.; Viruela-Martín, P. M.; Ortí, E. *J. Chem. Phys.* **1992**, *97*, 8470.
(28) Schadt, M. *J. Chem. Phys.* **1979**, *71*, 2336.

from −5.66 eV to −5.44 eV in passing from benzo-TCNQ to **9a**. The HOMO of benzo-TCNQ is also spread over the TCNQ moiety and should be correlated with the HOMO-1 of **9a**. This orbital is stabilized by the same energy amount (0.22 eV) the LUMO is destabilized. The VEH results therefore predict that the lowest-energy absorption band of benzo-TCNQ (3.04 eV) shifts to higher energies in **9a** (3.48 eV) and justify the hypsochromic shift observed experimentally for this absorption band in going from benzo-TCNQ (390 nm, 3.18 eV)[20c,29] to **9a** (360 nm, 3.44 eV). This absorption band is calculated to be polarized along the long molecular axis (y) for compounds **7** and **8**, similarly to that found for naphthoquinone derivatives,[15] and along the short axis z for compounds **9** and **10**. Figure 8 also shows the fact that the HOMO of **9a** has no correspondence in benzo-TCNQ. This molecular orbital is furnished by the donor unit and gives rise to the appearance of the extra charge-transfer band.

The same electronic structure trends discussed for **9a** are also found for compounds **9b** and **10**. As can be seen from Table 1, the substitution of one sulfur bridge by an oxygen produces a bathochromic shift of the charge transfer band passing from 515 nm (2.41 eV) for **9a** to 594 nm (2.09 eV) for **10a**. The theoretical calculations fail in predicting this shift (an energy of 2.53 eV is calculated for the HOMO → LUMO transition of **10a**) due to a well-known shortcoming of the oxygen parameterization used in VEH method.[30] In contrast, the theoretical results correctly predict the additional bathochromic shift induced by the introduction of the methyl substituents (see Table 1). The introduction of one methyl group in positions R_2 (**10b**) or R_3 (**10c**) induces a small lowering (0.03−0.04 eV) of the energy of the charge-transfer band due to the destabilization of the HOMO produced by the electron-releasing effect of the methyl group. The additional shift (0.06 eV) induced by a second methyl group in position R_1 (**10d**) should be ascribed to the planarization of the donor part of the molecule that this group produces (see Table 3). This planarization reinforces the antibonding interaction between the heteroatom bridges and the adjacent carbons and destabilizes the HOMO (see Figure 7).

Geometric and Electronic Structure of Oxidized and Reduced Compounds. The cyclic voltammetric data presented in Table 2 provide very similar values for the first oxidation potential of compounds **7a** (1.41 V) and **9a** (1.39 V). This result can be understood by considering that from the electronic structure standpoint oxidation involves removing an electron from the HOMO. As displayed in Figure 7, this orbital is localized on the donor moiety and similar oxidation potentials have therefore to be expected for compounds showing the same chemical structure for this part of the molecule like in **7a** and **9a**. This is also the case for compounds **8a** and **10a**, for which the donor unit is a benzooxathiin ring, and similar oxidation potentials (1.52 and 1.57 V, respectively) are found from electrochemical measurements. Electrochemical data also predict an increase of the oxidation potential in passing from **7a** to **8a** (0.11 V) or from **9a** to **10a** (0.15 V). This increase is due to the substitution of one sulfur bridge by a more electronegative oxygen atom in **8a** and **10a**, the variations measured being in fact smaller than that reported when replacing both sulfur bridges (0.35 V).[15]

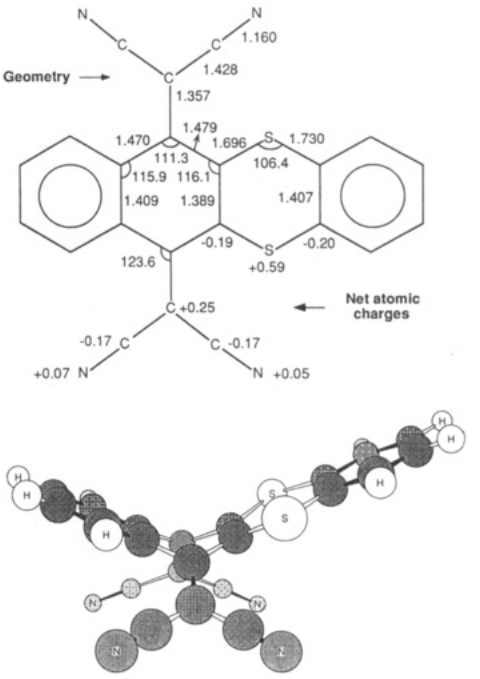

Figure 9. PM3-optimized geometry and net atomic charges (in e) calculated for the cation of **9a**. Bonds are in Å and angles in degrees. Only the values of the most relevant parameters are indicated. C_s symmetry has been assumed.

The effects of oxidation on the geometric and electronic structure are summarized in Figure 9 which shows the PM3-optimized geometry and net atomic charges calculated for the cation of **9a**. The inner benzodithiin ring is the part of the molecule most affected by oxidation. In accord with the fact that the HOMO is mainly localized on sulfur atoms (Figure 7), most of the charge is extracted from these atoms passing from a net charge of +0.24e in the neutral molecule to +0.59e in the cation, i.e., +0.70e are extracted from the sulfur atoms. By comparison to the neutral molecule, the benzodithiin ring therefore presents remarkable structural changes such as the shortening of the S1–C2 and S1–C18 bonds (from 1.751 and 1.765 Å to 1.696 and 1.730 Å, respectively) and the lengthening of the C2–C11 bond (from 1.360 to 1.389 Å), but certainly the main effect is the planarization of the ring. A value of 184.0° is calculated for angle β compared with the value of 202.8° obtained for the neutral molecule. All these changes determine a clear gain of aromaticity of the benzodithiin ring which is in fact the factor that makes feasible the obtention of stable radical cations. The rest of the molecular structure remains almost unaffected upon oxidation. The distortions from planarity of the TCNQ units ($\alpha = 132.7°$, $\gamma = 46.1°$) are similar to those calculated for the neutral molecule ($\alpha = 134.6°$, $\gamma = 43.9°$) and the outer benzene rings preserve their aromaticity.

Similarly to oxidation, reduction implies the introduction of an electron in the LUMO and lower reduction potentials could be expected for compounds with more stable LUMOs. This is actually the trend observed for quinones **7a** and **8a** for which the VEH method predicts a destabilization of the LUMO (0.13 eV) in accord with the slight increase of the first reduction potential (0.06 eV). This effect is not seen for TCNQ derivatives due to the mixing of the first two reduction potentials (Table 2).

(29) Chatterjee, S. *J. Chem. Soc. B.* **1967**, 1170.
(30) Eckhardt, H.; Shacklette, L. W.; Jen, K. Y.; Elsenbaumer, R. L. *J. Chem. Phys.* **1989**, *91*, 1303.

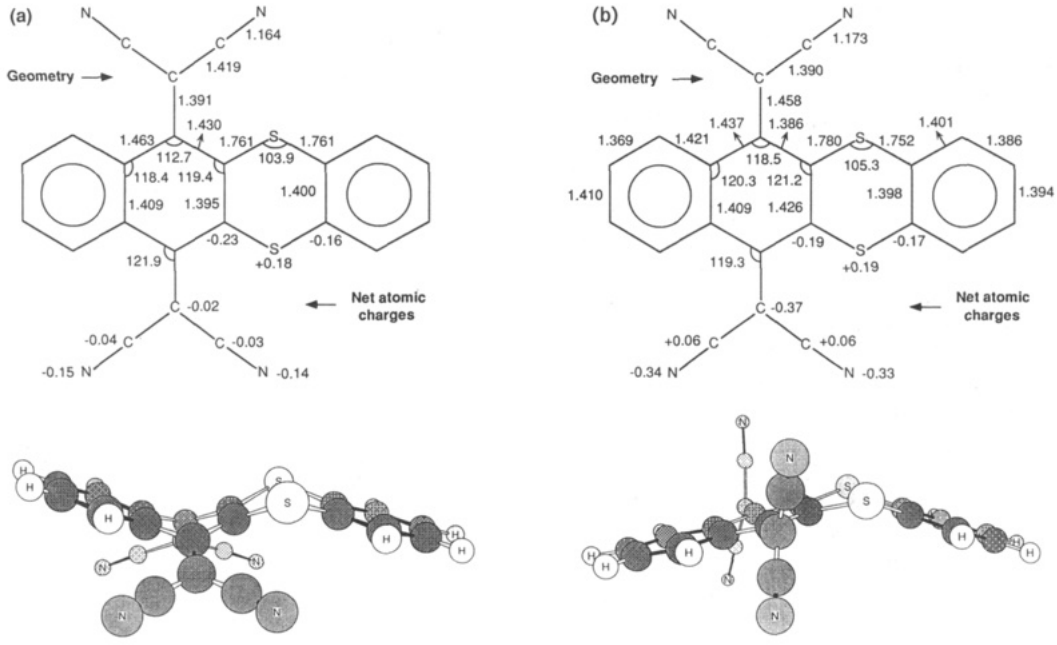

Figure 10. PM3-optimized geometry and net atomic charges (in e) calculated for the anion (a) and dianion (b) of **9a**. Bonds are in Å and angles in degrees. Only the values of the most relevant parameters are indicated. C_s symmetry has been assumed.

Since the LUMO is delocalized over the TCNQ moiety, the reduction process to form the anion and the dianion mainly affects this part of the molecule. This is illustrated in Figure 10 in which the PM3-optimized geometry and net atomic charges calculated for the anion and the dianion of **9a** are displayed. The introduction of the first electron to form the anion reduces the distortions from planarity of the TCNQ moiety in **9a**. The α angle increases to 142.8° and the γ angle decreases to 28.7° compared with the 134.6° and 43.9° values obtained for the respective angles in neutral **9a**. Furthermore, these changes are accompanied by a reduction of the quinoid character of the TCNQ ring. C3—C2,C4 and C10—C9,C11 single bonds are shortened and C2—C11, C3—C19, and C10—C24 double bonds are lengthened. These trends are more pronounced for the dianion, and the introduction of the second electron completes the process of aromatization of the TCNQ ring. Now the C3—C19 and C10—C24 bonds have a marked single character (1.458 Å), and the steric interactions between the cyano substituents and the CH groups and sulfur atoms in *peri* positions are more readily alleviated by twisting the dicyanomethylene groups out of the aromatic plane (Figure 10b) rather than by bending the TCNQ ring. This ring is therefore completely planar and forms with the adjacent benzene ring an aromatic naphthalene unit. This marked evolution of the TCNQ moiety to adopt an aromatic structure upon reduction clearly facilitates the formation of stable radical anions and dianions.

In order to provide a better understanding of the reduction process for the TCNQ derivatives **9** and **10**, we have calculated the evolution of the geometric and electronic structure of the parent TCNQ molecule upon reduction. Figure 11 summarizes the PM3-optimized geometries and net atomic charges obtained for neutral TCNQ and its anion and dianion.

As illustrated in Figure 11a, the charging process induces an aromatization of the TCNQ molecule similar to that discussed for **9a**, the only difference being that no distortion from planarity is found for TCNQ. Figure

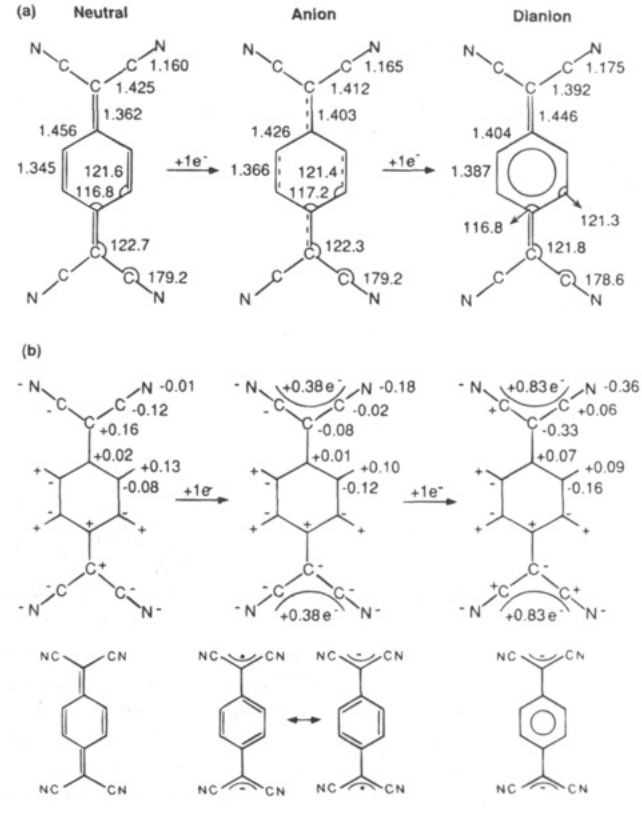

Figure 11. (a) PM3-optimized geometry and (b) net atomic charges (in e) calculated for neutral TCNQ and its anion and dianion. Bonds are in Å and angles in degrees. D_{2h} symmetry has been assumed.

11b shows how the extra electrons are accommodated in the dicyanomethylene units, the extra negative charges taken by each $C(CN)_2$ unit (0.83e) in the dianion being in fact equal to those calculated for **9a** (0.83e). What is then the difference between TCNQ and compounds **9** and **10** that justifies the fact that the latter presents a unique two-electron step in the reduction process to the dianion? The answer should be found in the different structure

found for TCNQ and for the TCNQ moiety in **9** and **10**, i.e., in the lack of planarity the TCNQ ring shows in the latter. The distortion from planarity determines that the LUMO of **9a** (−5.44 eV) and **10a** (−5.34 eV) are calculated to be 0.79 and 0.89 eV higher in energy than the LUMO of TCNQ (−6.23 eV). This destabilization signifies that reduction takes place less easily than in TCNQ, i.e., that the first reduction potential of compounds **9** and **10** should be shifted to a more negative range. This additional difficulty in reducing **9** and **10** is supported by the fact that the acceptor $C(CN)_2$ units in the anion of **9a** accumulate an extra negative charge of 0.56e significantly lower than the 0.76e calculated for the anion of TCNQ. Furthermore, the anion of **9a** remains to be nonplanar and therefore less aromatic than the anion of TCNQ. The second reduction potential should be expected to have similar values in TCNQ and **9a** since the dianion presents for both systems a similar aromatic structure and identical charge accumulation on the dicyanomethylene units (0.83e each). These trends explain the mixing of the first and second reduction potentials in compounds **9** and **10**.

Summary and Conclusions

We have described the synthesis of novel derivatives **9** and **10** of the widely-investigated TCNQ acceptor molecule that incorporates heteroatomic donor units. The resulting single-component donor–acceptor compounds present a low-energy absorption band in their UV–vis spectra that corresponds to an intramolecular charge-transfer between the donor and acceptor moieties. They provide stable radical cations upon oxidation and lead to the dianion in a unique two-electron process upon reduction. The structural X-ray crystallographic analysis performed on single crystals of **10d** shows that molecules are not planar, both the donor benzodithiin (**9**) or benzooxathiin (**10**) rings and the acceptor TCNQ moiety adopting a boat conformation. Molecules are packed in vertical stacks where donor and acceptor moieties alternately change their position. In agreement with this aggregation in mixed stacks [...(A–D)(D–A)(A–D)...] the electrical conductivity measured for compound **10c** displays a semiconducting behavior.

Molecular orbital calculations have been performed to help the understanding of the experimental results. The PM3 equilibrium geometric structures calculated for **9** and **10** show that these compounds are severely distorted from planarity. The trends observed for these distortions are rationalized in terms of nonbonding interactions and explain the conformation adopted by the molecules in the crystal. The electronic structures of compounds **9** and **10** have been studied using the nonempirical VEH method. This method predicts that the electronic charge density in the HOMO is localized mainly on the benzodithiin (**9**) or benzooxathiin (**10**) rings, while in the LUMO is found mostly on the TCNQ environment. The HOMO → LUMO transition therefore corresponds to an electronic transfer from the donor to the acceptor moieties supporting the intramolecular charge-transfer nature of the lowest-energy absorption band observed experimentally. This band is calculated to be polarized along the short molecular axis.

The stability of oxidized and reduced compounds have been studied by calculating the evolution of the geometric and electronic structures on the charging process. PM3 calculations show that both oxidation and reduction induce a clear gain of aromaticity. Since the HOMO is spread over the donor moiety, the benzodithiin (**9**) or benzooxathiin (**10**) rings are planarized upon oxidation. In the same way, the LUMO is localized on the acceptor environment and the TCNQ moiety is aromatized upon reduction. The aromatization of the TCNQ moiety allows for the rotation of the dicyanomethylene units that alleviates the steric interactions and, as a consequence, permits the planarization of the TCNQ ring. These structural modifications justify the obtention of a single two-electron wave to the dianion when reducing these kind of compounds.

Experimental Section

All melting points were measured on a Gallenkamp melting point apparatus and are uncorrected. IR spectra were recorded on a Perkin-Elmer 257 spectrometer. UV Spectra were recorded on a Perkin-Elmer Lambda 3 instrument. ^1H NMR spectra were determined with a Varian XL-300 spectrometer, and elemental analyses were performed on a Perkin-Elmer CHN 2400 apparatus.

Cyclovoltammetric measurements were performed on a EG & PAR Versastat potentiostat using 250 Electrochemical Analysis software. A Metrohm 6.0804.C10 glassy carbon electrode was used as indicator electrode in voltammetric studies.

An HP 4192 Impedance analyzer was used for conductivity measurements with variable frequency with silver paint contacts.

2,3-Dichloro-1,4-naphthoquinone, 1,2-benzenedithiol, 3,4-dimercaptotoluene, 2-aminophenol, 2-amino-*p*-cresol, 6-amino-*m*-cresol, 6-amino-2,4-dimethylphenol, potassium ethyl xanthate, malononitrile, and $TiCl_4$ were obtained from commercial sources and used without further purification. *o*-Thiophenols were synthesized by following the method previously reported in the literature.[17]

X-ray Crystallographic Measurements: Crystal data for compound 10d: $C_{24}H_{12}N_4OS$, MW = 404.445, orthorombic, $P2_1$, a = 18.977(2) Å, b = 8.118(1) Å, c = 12.836(1) Å, V = 1977.5(4) Å^3, z = 4, D_c = 1.36 g/mL, $F(000)$ = 832, μ = 16.00 cm^{-1}. Refined cell parameters were obtained from setting angles of 60 reflections. A prismatic brown crystal (0.30 × 0.13 × 0.10 mm) was used for the analysis.[49]

Data Collection. Automatic four circle diffractometer Philips PW 1100 with graphite-oriented monochromated Cu–Kα radiation. The intensity data were collected using the $\omega/2\theta$ scan mode between $2 < \theta < 65°$; two standard reflections were measured every 90 min with no intensity variation. A total of 1982 reflections were measured and 1359 were considered as observed ($I > 3\sigma(I)$ criterium). The data were corrected for Lorentz and Polarization effects.

Structure Solutions and Refinement. The structure was solved by direct methods using SIR 88[31] and DIRDIF92.[32] H atoms were calculated and included in a mixed refinement; isotropic thermal parameters of these atoms were considered as fixed contributors. A convenient weighting scheme was applied to obtain flat dependence in $\langle w\Delta^2F\rangle$ vs $\langle F_0\rangle$ and $\langle \sin\theta/\lambda\rangle$.[33] Final R (Rw) value was 5.4 (6.4). Atomic scattering factors for the compound were taken from *Interna-*

(31) Cascarano, G.; Giacovazzo, C. Dip. Geomineralogico-Univ. of Bari. Burla, M. G.; Polidori, G. Dip. Scienze de la terra-Univ. of Perugia. Camalli, M.; Spagna, R. Ist. Strutt. Chimica CNR-Monterotondo Stazione, Roma. Viterbo, D. Dip. di Chimica, Univ. della Calabria, Consenza. SIR88., **1988**.

(32) The DirDif Program System. Beurskens, P. T.; Admiral, G.; Behm, H.; Beurskens, G.; Bosman, W. P.; García-Granda, S.; Gould, R. O.; Smykalla, C. *Zeitsch. Krist.* **1990**, *4*, 99.

(33) Martínez-Ripoll, M; Cano, F. H. PESOS. A computer program for the automatic treatment of weighting schemes. Instituto Rocasolano C.S.I.C. Serrano 119, 28006 Madrid, Spain.

tional Tables for X-Ray Crystallography,[34] and calculations were performed using XRAY80,[35] XTAL,[36] HSEARCH,[37] and PARST.[38]

Computational Method. The equilibrium geometries of quinones **7** and **8** and TCNQ derivatives **9** and **10** were calculated by means of the MNDO-PM3 (modified neglect of diatomic overlap, parametric method no. 3) semiempirical method[39] as implemented in the MOPAC-6.0 system of programs.[40] The MNDO-PM3 method corresponds to a reparameterization of the MNDO approach[41] in which the AM1 (Austin model 1) form of the core–core interaction is used.[42] The suitability of the PM3 method to obtain reliable geometry estimates for organic compounds has been previously established.[40] With respect to MNDO, the PM3 technique provides a much improved description of the interactions taking place between nonbonded atoms, e.g., hydrogen bonding or steric interactions. The latter are specially important for the set of molecules studied in this work since they determine the planarity or nonplanarity of the system.

The geometry of neutral molecules and dianions was optimized within the restricted Hartree–Fock (RHF) formalism, while the spin-unrestricted Hartree–Fock (UHF)[43] approximation where electrons with different spins occupy different sets of orbitals was used for single-charged cations and anions. In all the calculations, the gradient norm achieved was less than 0.05. The stationary points calculated for the parent TCNQ derivatives **9a** and **10a** were characterized by calculating force constants.[44] The two structures displayed in Figure 6 for **9a** and that obtained for **10a** are shown to be really minima since all the force constants are calculated to be positive.

The electronic structure of compounds **7** to **10** was investigated using the nonempirical valence effective Hamiltonian (VEH) pseudopotential technique.[45] This technique takes only into account the valence electrons and is based on the use of an effective Fock Hamiltonian parametized to reproduce the results of *ab initio* Hartree–Fock calculations without performing any self-consistent-field (SCF) process or calculating any bielectronic integral. The VEH method therefore is completely nonempirical and constitutes an especially useful tool to deal with large molecular or crystalline systems, since it yields one-electron energies of *ab initio* double-ζ quality at a reasonable computer cost. All the VEH calculations were performed using the atomic potentials previously optimized for hydrogen, carbon, oxygen, and sulfur atoms.[46] The validity of the VEH approach to study the electronic structure of large π-electronic molecular systems has been widely illustrated in previous works.[47,48]

Synthesis of Quinones 7 and 8. General Procedure. To a stirred solution of the corresponding *o*-benzenedithiol (**4**) (3.3 mmol) or *o*-thiophenol (**5**) (15 mmol) in 25 mL of dry pyridine at 100 °C and argon atmosphere was added 2,3-dichloro-1,4-naphthoquinone (**6**) (1.3 mmol for **4** and 7.5 mmol for **5**). After being stirred for 6 h at this temperature, the reaction mixture was left at room temperature overnight. The solid precipitated was collected by filtration and washed with methanol and then ethyl ether. Further purification was accomplished by recrystallization from acetonitrile.

Benzo[*b*]naphtho[2,3-*e*][1,4]dithiin-6,11-quinone (7a): yield 73%; mp 288–290 °C (from acetonitrile); ^{1}H-NMR (300 MHz, $CDCl_3$) δ 8.13–8.10 (m, 2 H), 7.75–7.72 (m, 2 H), 7.32–7.22 (m, 4 H, Ar-H); IR (KBr) 1670, 1585, 1530, 1450, 1275, 1140, 805, 760, 700 cm^{-1}; UV ($CHCl_3$) λ_{max} (log ϵ) 542 (2.94), 349 (3.76), 284 (4.21), 244 (4.45); MS *m/e* 298 (M^++ 2, 11), 296 (M^+, 100), 268 (10), 240 (25), 208 (8), 163 (10), 120 (30), 76 (29). Anal. Calcd for $C_{16}H_8O_2S_2$: C, 64.84; H, 2.73. Found: C, 64.84; H, 2.78.

2-Methylbenzo[*b*]naphtho[2,3-*e*][1,4]dithiin-6,11-quinone (7b): yield 78%; mp 268–270 °C (from acetonitrile); ^{1}H-NMR (300 MHz, $CDCl_3$) δ 8.11–8.08 (m, 2 H), 7.73–7.70 (m, 2 H), 7.15–7.13 (d, 1 H), 7.09–7.08 (s, 1 H), 7.02–7.0 (s, 1 H), 2.28 (s, 3 H, Me); IR (KBr) 1665, 1590, 1530, 1470, 1450, 1280, 1140, 805, 700 cm^{-1}; UV ($CHCl_3$) λ_{max} (log ϵ) 558 (2.95), 350 (3.75), 288 (4.26), 244 (4.49); MS *m/e* 312 (M^+ + 2, 12), 310 (M^+, 100), 282 (17), 254 (30), 221 (14), 76 (24), 69 (15), 50 (15). Anal. Calcd for $C_{17}H_{10}O_2S_2$: C, 65.78; H, 3.25. Found: C, 65.71; H, 3.25.

Benzo[*b*]naphtho[2,3-*e*][1,4]oxathiin-6,11-quinone (8a): yield 82%; mp 256–258 °C (from acetonitrile); ^{1}H-NMR (300 MHz, $CDCl_3$) δ 8.15–8.12 (m, 1 H), 8.09–8.06 (m, 1 H), 7.77–7.70 (m, 2 H), 7.04–6.96 (m, 4 H); IR (KBr) 1660, 1640, 1605, 1585, 1560, 1465, 1440, 1290, 1245, 1210, 1010, 910, 850, 750, 700 cm^{-1}; UV ($CHCl_3$) λ_{max} (log ϵ) 548 (2.97), 342 (3.62), 285 (4.34), 240 (4.33); MS *m/e* 282 (M^+ + 2, 16), 280 (M^+, 100), 252 (14), 224 (53), 195 (31), 163 (15), 152 (48), 76 (84). Anal. Calcd for $C_{16}H_8O_3S$: C, 68.57; H, 2.88. Found: C, 68.62; H, 2.99.

2-Methylbenzo[*b*]naphtho[2,3-*e*][1,4]oxathiin-6,11-quinone (8b): yield 91%; mp 244–246 °C (from acetonitrile); ^{1}H-NMR (300 MHz, $CDCl_3$) δ 8.12–8.09 (m, 1 H), 8.06–8.03 (m, 1 H), 7.73–7.70 (m, 2 H), 6.84 (s, 1 H), 6.82–6.81 (d, 2 H), 2.24 (s, 3 H, Me); IR (KBr) 1670, 1650, 1610, 1595, 1565, 1490, 1300, 1260, 1240, 1200, 860, 715 cm^{-1}; UV ($CHCl_3$) λ_{max} (log ϵ) 560 (2.98), 346 (3.61), 286 (4.38), 240 (4.19); MS *m/e* 296 (M^+ + 2, 7), 294 (M^+, 100), 266 (4), 238 (13), 104 (13), 76 (25). Anal. Calcd for $C_{17}H_{10}O_3S$: C, 69.40; H, 3.40. Found: C, 69.19; H, 3.37.

3-Methylbenzo[*b*]naphtho[2,3-*e*][1,4]oxathiin-6,11-quinone (8c): yield 87%; mp 230–232 °C (from acetonitrile); ^{1}H-NMR (300 MHz, $CDCl_3$) δ 8.14–8.11 (m, 1 H), 8.08–8.05 (m, 1 H), 7.76–7.71 (m, 2 H), 6.89 (s, 2 H), 6.77 (s, 1 H), 2.23 (s, 3 H, Me); IR (KBr) 1670, 1645, 1610, 1590, 1570, 1480, 1300, 1250, 1230, 1210, 1010, 910, 850, 710 cm^{-1}; UV ($CHCl_3$) λ_{max} (log ϵ) 558 (2.92), 345 (3.63), 291 (4.29), 241 (4.19); MS *m/e* 296 (M^+ + 2, 9), 294 (M^+, 100), 266 (4), 238 (15), 104 (11), 76 (24). Anal. Calcd for $C_{17}H_{10}O_3S$: C, 69.40; H, 3.40. Found: C, 69.42; H, 3.15.

1,3-Dimethylbenzo[*b*]naphtho[2,3-*e*][1,4]oxathiin-6,11-quinone (8d): yield 73%; mp 260–262 °C (from acetonitrile); ^{1}H-NMR (300 MHz, $CDCl_3$) δ 8.12–8.05 (m, 2 H), 7.76–7.69 (m, 2 H), 6.74 (s, 1 H), 6.61 (s, 1 H), 2.29 (s, 3 H, Me), 2.18 (s, 3 H, Me); IR (KBr) 1670, 1650, 1620, 1595, 1575, 1470, 1330, 1300, 1210, 1150, 925, 860, 710; UV ($CHCl_3$) λ_{max} (log ϵ) 565 (2.93), 347 (3.66), 284 (4.29), 242 (4.39); MS *m/e* 310 (M^+ + 2,

(34) *International Tables for X-Ray Crystallography*; Birmingham Press: Birmingham, 1974; Vol. IV.
(35) Hall, S. R.; Stewart, J. M. XTAL System, University of Western Australia, Perth, Australia, 1990.
(36) Stewart, J. M.; Kundell, F. A.; Baldwin, J. C. The X-Ray76 Computer Science Center, University of Maryland, College Park, Maryland, EEUU, 1976.
(37) Fayos, J.; Martínez-Ripoll, M. HSEARCH. A computer program for the geometric calculations of H atom Coordinates; Instituto Rocasolano, C.S.I.C., Madrid, Spain, 1978.
(38) Nardeli, M. PARST, *Comput. Chem.* **1983**, *7*, 95–98.
(39) Stewart. J. J. P. *J. Comput. Chem.* **1989**, *10*, 209; **1989**, *10*, 221.
(40) Stewart, J. J. P. MOPAC: A General Molecular Orbital Package (Version 6.0), QCPE **1990**, *10*, 455.
(41) Dewar, M. J. S.; Thiel, W. *J. Am. Chem. Soc.* **1977**, *99*, 4899.
(42) Dewar, M. J. S.; Zoebisch, E. G.; Healy, E. F.; Stewart, J. J. P. *J. Am. Chem. Soc.* **1985**, *107*, 3902.
(43) Pople, J. A.; Nesbet, R. K. *J. Chem. Phys.* **1954**, *22*, 571.
(44) McIver, J. W.; Komornicki, A. *Chem Phys. Lett.* **1971**, *10*, 303. McIver, J. W.; Komornicki, A. *J. Am. Chem. Soc.* **1972**, *94*, 2625.
(45) Nicolas, G.; Durand, Ph. *J. Chem. Phys.* **1979**, *70*, 2020; **1980**, *72*, 453. André, J. M.; Burke, L. A.; Delhalle, J.; Nicolas, G.; Durand, Ph. *Int. J. Quantum Chem. Symp.* **1979**, *13*, 283. Brédas, J. L.; Chance, R. R.; Silbey, R.; Nicolas, G., Durand, Ph. *J. Chem. Phys.* **1981**, *75*, 255.
(46) André, J. M.; Brédas, J. L.; Delhalle, J.; Vanderveken, D. J.; Vercauteren, D. P.; Fripiat, J. G. In *Modern Techniques in Computational Chemistry: MOTECC-90*; Clementi, E., Ed.; Escom: Leiden, The Netherlands, 1990; p 745. Brédas, J. L.; Thémans, B.; André, J. M. *J. Chem. Phys.*, **1983**, *78*, 6137.
(47) Ortí, E.; Brédas, J. L. *J. Chem. Phys.* **1988**, *89*, 1009. Ortí, E.; Brédas, J. L. *Chem. Phys. Lett.* **1989**, *164*, 247. Ortí, E.; Brédas, J. L.; Clarisse, C. *J. Chem. Phys.* **1990**, *92*, 1228. Ortí, E.; Piqueras, M. C.; Crespo, R.; Brédas, J. L. *Chem. Mater.* **1990**, *2*, 110.
(48) Viruela-Martín, R.; Viruela-Martín, P. M.; Ortí, E. *J. Chem. Phys.* **1992**, *96*, 4474.
(49) The author has deposited atomic coordinates for **10d** with the Cambridge Crystallographic Data Centre. The coordinates can be obtained, on request, from the Director, Cambridge Crystallographic Data Centre, 12 Union Road, Cambridge, CB2 1EZ, UK.

7), 308 (M^+, 100), 280 (3), 275 (4), 252 (7), 76 (18). Anal. Calcd For $C_{18}H_{12}O_3S$: C, 70.12; H, 3.89. Found: C, 69.89; H, 3.86.

Condensation of Quinones 7 with Malononitrile. General Procedure. To a solution of the corresponding quinone (**7**) (1 mmol) and malononitrile (2.5 mmol) in 30 mL of dry CH_2Cl_2 were added $TiCl_4$ (2.5 mmol) followed by dry pyridine (5 mmol) dropwise under argon atmosphere. The reaction mixture was stirred for 24 h (monitored by TLC), and then malononitrile (1 mmol), $TiCl_4$ (1 mmol), and pyridine (2 mmol) were added. The reaction mixture was stirred for another additional 12 h. The black solid that precipitated was filtered off and washed with plenty of water. By concentrating the mother liquors, a second crop of product was obtained. By fractional recrystallization from acetonitrile, compound **9** was obtained first. The monocondensation isomers (**11**) were obtained as a black solid from the mother liquors.

Monocondensated compounds (**11**) could also be obtained as the major product by following the above general procedure, but using a quinone:malononitrile ratio of 1:1.5 and a reaction time of 16 h. Thus, compounds **11** were obtained in 60–70% yield.

13,13,14,14-Tetracyanobenzo[*b*]naphtho[2,3-*e*][1,4]dithiin-6,11-quinodimethane (9a): yield 40%; mp > 300 °C (from acetonitrile); ^{1}H-NMR (300 MHz, $CDCl_3$) δ 8.29–8.25 (q, 1 H), 8.14–8.11 (q, 1 H), 7.77–7.72 (m, 2 H), 7.52–7.49 (q, 1 H), 7.34–7.31 (m, 1 H), 7.25–7.22 (m, 2 H); IR (KBr) 2220, 1585, 1540, 1500, 1450, 1275, 750; UV ($CHCl_3$) λ_{max} (log ϵ) 515 (3.35), 360 (4.15), 287 (3.90), 261 (3.86), 241 (4.25); MS *m/e* 392 (M^+, 100). Anal. Calcd for $C_{22}H_8N_4S_2$: C, 67.35; H, 2.04; N, 14.28. Found: C, 67.14; H, 2.30; N, 14.54.

6-(Dicyanomethylene)benzo[*b*]naphtho[2,3-*e*][1,4]dithiin-11-one (11a): yield 23%; mp >300 °C (from acetonitrile); IR (KBr) 2220, 1670, 1590, 1530, 1500, 1450, 1420, 1275, 750 cm^{-1}; MS *m/e* 346 (M^+ + 2, 7), 344 (M^+, 100), 316 (16), 296 (83), 268 (14), 240 (93), 208 (18), 163 (19), 120 (16), 76 (32), 50 (35). Anal. Calcd for $C_{19}H_8N_2S_2$: C, 66.28; H, 2.32; N, 8.14. Found: C, 66.14; , 2.30; N, 8.54.

13,13,14,14-Tetracyano-2-methylbenzo[*b*]naphtho[2,3-*e*][1,4]dithiin-6,11-quinodimethane (9b): yield 47%; mp >300 °C (from acetonitrile); ^{1}H-NMR (300 MHz, $CDCl_3$) δ 8.26–8.23 (m, 2 H), 7.75–7.72 (m, 2 H), 7.59–7.57 (d, 1 H), 7.50 (s, 1 H), 7.25–7.24 (d, 1 H), 2.40 (s, 3 H, Me); IR (KBr) 2220, 1580, 1545, 1500, 1460, 1270, 810, 750 cm^{-1}; UV ($CHCl_3$) λ_{max} (log ϵ) 528 (3.52), 368 (4.32), 288 (4.16), 266 (4.15), 241 (4.38); MS *m/e* 408 (M^+ + 2, 14), 406 (M^+, 100), 391 (7), 379 (30), 358 (15), 121 (18), 77 (23), 69 (25). Anal. Calcd for $C_{23}H_{10}N_4S_2$: C, 67.96; H, 2.48; N, 13.77. Found: C, 67.62; H, 2.77; N, 13.74.

11-Dicyanomethylene-2-methylbenzo[*b*]naphtho[2,3-*e*][1,4]dithiin-6-one and 6-dicyanomethylene-2-methylbenzo[*b*]naphtho[2,3-*e*][1,4]dithiin-11-one (11b): yield 19%; mp >300 °C (from acetonitrile); IR (KBr) 2215, 1665, 1595, 1540, 1520, 1470, 1280, 1150, 800, 790, 740, 700 cm^{-1}. Anal. Calcd for $C_{20}H_{10}N_2OS_2$: C, 67.00; H, 2.79; N, 7.82. Found: C, 66.75; H, 2.74; N, 7.25.

Condensation of Quinones 8 with Malononitrile. General Procedure. To a solution of the corresponding quinone (**8**) (1 mmol) and malononitrile (3.5 mmol) in 40 mL of dry CH_2Cl_2 were added $TiCl_4$ (3.5 mmol) followed by dry pyridine (7 mmol) dropwise under argon atmosphere. The reaction mixture was stirred for 48 h (monitored by TLC), and a solid precipitated. The solvent was evaporated under vacuum and the residual solid was vigorously stirred with HCl (10%). The resulting solid was washed several times with plenty of water and dried. The product obtained was identified as the tetracyano derivative (**10**) slightly contaminated with the dicyano-derivative (**12**). Further purification was accomplished by recrystallization from acetonitrile.

Monocondensated compounds (**12**) can also be obtained as the major product by following the above general procedure, but using a quinone:malononitrile ratio of 1:2 and a reaction time of 24 h. Thus, compounds **12a** and **12c** could be obtained.

13,13,14,14-Tetracyanobenzo[*b*]naphtho[2,3-*e*][1,4]oxathiin-6,11-quinodimethane (10a): yield 37%; mp >300 °C; ^{1}H-NMR (300 MHz, $CDCl_3$) δ 8.70–8.42 (d, 1 H), 8.32–8.27 (d, 1 H), 7.75 (s, 2 H), 7.3–7.04 (m, 4 H); IR (KBr) 2220, 1580, 1530, 1470, 1440, 1350, 1260, 1220, 760 cm^{-1}; UV ($CHCl_3$) λ_{max} (log ϵ) 594 (3.42), 373 (4.25), 293 (4.18), 240 (4.26). Anal. Calcd for $C_{22}H_8N_4OS$: C, 70.21; H, 2.12; N, 14.89. Found: C, 70.11; H, 2.07; N, 14.63.

13,13,14,14-Tetracyano-2-methylbenzo[*b*]naphtho[2,3-*e*][1,4]oxathiin-6,11-quinodimethane (10b): yield 41%; mp >300 °C (from acetonitrile); ^{1}H-NMR (300 MHz, $CDCl_3$) δ 8.46–8.43 (m, 1 H), 8.29–8.26 (m, 1 H), 7.76–7.73 (m, 2 H), 7.09–7.04 (m, 3 H), 2.35 (s, 3 H, Me); IR (KBr) 2215, 1590, 1540, 1490, 1410, 1350, 1270, 1220, 815, 770 cm^{-1}; UV ($CHCl_3$) λ_{max} (log ϵ) 606 (3.45), 379 (4.41), 289 (4.17), 253 (4.14), 239 (4.22). Anal. Calcd for $C_{23}H_{10}N_4OS$: C, 70.77; H, 2.56; N, 14.36. Found: C, 70.56; H, 2.54; N, 14.32.

13,13,14,14-Tetracyano-3-methylbenzo[*b*]naphtho[2,3-*e*][1,4]oxathiin-6,11-quinodimethane (10c): yield 46%; mp >300 °C; ^{1}H-NMR ($CDCl_3$) δ 8.56–8.53 (m, 1 H), 8.24–8.21 (m, 1 H), 7.76–7.71 (m, 2 H), 7.38–7.34 (d, 1 H), 7.15–7.12 (d, 1 H), 7.08 (s, 1 H), 2.32 (s, 3 H, Me); IR (KBr) 2215, 1590, 1540, 1490, 1410, 1350, 1270, 1220, 815, 770; UV ($CHCl_3$) λ_{max} (log ϵ) 603 (3.43), 374 (4.55), 293 (4.40), 240 (4.43). Anal. Calcd for $C_{23}H_{10}N_4OS$: C, 70.77; H, 2.56; N, 14.36. Found: C, 70.53; H, 2.54; N, 14.30.

13,13,14,14-Tetracyano-1,3-dimethylbenzo[*b*]naphtho-[2,3-*e*][1,4]oxathiin-6,11-quinodimethane (10d): Yield 52%; mp >300 °C (from acetonitrile); ^{1}H-NMR ($CDCl_3$) δ 8.35–8.32 (m, 1 H), 8.25–8.22 (m, 1 H), 7.71–7.68 (m, 2 H), 6.85 (s, 1 H), 6.71 (s, 1 H), 2.37 (s, 3 H, Me), 2.22 (s, 3 H, Me); IR (KBr) 2220, 1580, 1540, 1470, 1270, 1210, 760 cm^{-1}; UV ($CHCl_3$) λ_{max} (log ϵ) 621 (3.29), 382 (4.45), 287 (4.15), 242 (4.37). Anal. Calcd for $C_{24}H_{12}N_4OS$: C, 71.29; H, 2.97; N, 13.86. Found: C, 71.27; H, 2.97; N, 13.81.

6-(Dicyanomethylene)benzo[*b*]naphtho[2,3-*e*][1,4]oxathiin-11-one and 11-(dicyanomethylene)benzo[*b*]naphtho[2,3-*e*][1,4]oxathiin-6-one (12a): yield 26%; mp >300 °C (from acetonitrile); ^{1}H-NMR ($CDCl_3$) δ 8.61–8.58 (m, 1 H), 8.23–8.20 (m, 1 H), 7.80–7.70 (m, 2 H), 7.25–7.08 (m, 4 H); IR (KBr) 2215, 1650, 1530, 1475, 1320, 750. Anal. Calcd for $C_{19}H_8N_2O_2S$: C, 69.51; H, 2.44; N, 8.54. Found: C, 69.03; H, 2.39; N, 8.59.

6-(Dicyanomethylene)-3-methylbenzo[*b*]naphtho[2,3-*e*][1,4]oxathiin-11-one and 11-(dicyanomethylene)-3-methylbenzo[*b*]naphtho[2,3-*e*][1,4]oxathiin-6-one (12c): yield 34%; mp >300 °C (from acetonitrile); ^{1}H-NMR ($CDCl_3$) δ 8.60–8.58 (d, 1 H), 8.22–8.19 (d, 1 H), 7.76–7.71 (m, 2 H), 7.17–7.14 (d, 1 H), 6.96–6.93 (d, 1 H), 6.82 (s, 1 H); IR (KBr) 2210, 1650, 1600, 1550, 1480, 1200, 800, 770, 700 cm^{-1}. Anal. Calcd for $C_{20}H_{10}N_2O_2S$: C, 70.17; H, 2.92; N, 8.19. Found: C, 70.08; H, 2.89; N, 8.05.

Acknowledgment. This work has been supported by the DGICYT Projects PB92-0237, PB91-0935, and OP90-0042. The authors thank the CIUV (Centro de Informática de la Universitat de València) for the use of their computing facilities. One of the authors (J.L.S.) is indebted to U. Complutense de Madrid for a research fellowship.